

# Effect of Quasi-orthogonal Emission Modes on the Rotation Measures of Pulsars

R. Ramachandran & D. C. Backer

*Department of Astronomy, University of California, Berkeley, CA 94720-3411, USA;  
e-mail: ramach,dbacker@astro.berkeley.edu*

Joanna M. Rankin

*Physics Department, University of Vermont, Burlington, VT 05405 USA;  
email: joanna.rankin@uvm.edu*

J. M. Weisberg & K. E. Devine

*Department of Physics & Astronomy, Carleton College, Northfield, MN 55057;  
email: jweisber@carleton.edu*

## ABSTRACT

We report here the discovery of a significant source of systematic error in the rotation measure determinations of pulsars. Conventional analysis of high sensitivity polarimetric observations of PSR B2016+28 display variation of the rotation measure of  $\pm 15 \text{ rad m}^{-2}$  (around the mean value of  $-34.6 \text{ rad m}^{-2}$ ) across the pulse profile. Analysis of single pulse data shows that this variation is an artifact of the incoherent superposition of quasi-orthogonal polarisation modes along with the frequency dependence of relative strength and/or quasi-orthogonality of the modes. Quasi-orthogonal polarization is common among pulsars, and therefore this effect needs to be taken into account in the interpretation of pulsar rotation measures.

*Subject headings:* pulsars: polarisation – radiation mechanism: non-thermal – ISM: Magnetic field

## 1. Introduction

Pulsars play a major role in our understanding of interstellar magnetic field structure owing to measurements of Faraday rotation of the plane of linear polarization as a function of radio frequency introduced by the component of the field along the sight line in the warm interstellar medium ( $B_{\parallel}$ ). The standard definition of rotation measure (RM) in c.g.s. units is given by

$$\text{RM} = \frac{e^3}{2\pi m_e^2 c^4} \int_0^L n_e(l) B_{\parallel}(l) dl \quad (1)$$

where  $L$  is the distance to the pulsar from the observer,  $dl$  is the length element along the line of sight, and  $n_e$  is the free electron number den-

sity.  $e$  and  $m_e$  are the charge and the mass an electron, and  $c$  is the velocity of light in vacuum. The amount of rotation experienced by the intrinsic linear polarisation position angle of the source ( $\psi_o$ ) at a given wavelength ( $\lambda$ ) is expressed as

$$\psi - \psi_o = \text{RM} \lambda^2, \quad (2)$$

where  $\psi$  is the apparent linear polarisation position angle (PA) as seen by the observer. Several investigators in the past have measured RM values of pulsars (Manchester 1972; 1974; Hamilton et al. 1981; Hamilton & Lyne 1987; Rand & Lyne 1994; Qiao et al. 1995; Weisberg et al. 2003). Time dependence in the measured RM values<sup>1</sup> have also

<sup>1</sup>It is also important to compensate for the variable iono-

been noted against some pulsars like the ones in the Vela and Crab supernova remnants (Hamilton et al. 1977; Rankin et al. 1988). A positive RM means the direction of magnetic field is towards the observer, and a negative RM means otherwise. Using the measured values, detailed modelling of magnetic field structure has been carried out by several authors in the past (Thompson & Nelson 1980; Lyne et al. 1989; Indrani & Deshpande 1998; Han et al. 1999; 2002; Mitra et al. 2003). All of these galactic models based on pulsar RMs have a central assumption that the RM is completely determined by the interstellar medium, and that the magnetosphere of the pulsar, with all of its complexities, does not contribute significantly.

We show in this paper that a conventional RM analysis based on average pulse profiles leads to large variations of the RM across the pulse profile of PSR B2016+28. The conventional analysis requires some form of averaging to arrive at a single RM. Additional work that we are doing has shown that this effect occurs in other pulsars as well. In pulsars with significant RM variations across the pulse profile, there is a source of error that may not have been considered in past modeling of galactic magnetic fields.

Significant magneto-ionic propagation effects are not expected in pulsar magnetospheres owing to the ultra-relativistic nature of the plasma. Any large Faraday rotation within the emission region of the magnetosphere would lead to severe depolarisation across our band. The fact that pulsar radiation is highly polarised therefore shows that there is no significant Faraday rotation within the emission region. We are led then to look more closely at the data to determine the nature of the RM variations across the pulse.

We show in this work an improved method for RM determination when sufficient signal-to-noise ratio (S/N) allows detection of the pulsed radiation in single pulses. In this case, the orthogonal modes of polarization (e.g., Backer & Rankin 1980) can be identified, and the RM can be determined from each mode independently. If the modes were strictly orthogonal AND there was no jitter AND

---

spheric contribution to the measured RM values. As Manchester (1972) states, this contribution could be as high as some  $0.1$  to  $6 \text{ rad m}^{-2}$ , depending on the time of the day and the declination of the pulsar.

there was no frequency dependence of these properties, then this procedure would not be necessary. However, the PAs (position angles) at each longitude do display jitter and a slight degree of non-orthogonality (Gil, Snakowski & Stinebring 1991; Gil et al. 1992). We show in this work that the B2016+28 emission has a slight frequency dependence in the relative strengths and (or) amounts of non-orthogonality. This is the source of the pulse-longitude dependence of the RM in the conventional analysis. One does not have to appeal to strong, and unexpected, magneto-ionic propagation effects.

Most pulsars for which any amount of single pulse study exists show signs of orthogonal modes in their emission. The problem of origin of these modes has been addressed by several investigators (e.g., Melrose 1979; Petrova & Lyubarskii 2000; Radhakrishnan & Deshpande 2001; Petrova 2001). As they describe, the orthogonal mode could arise from the partial conversion of an original mode (ordinary) to the other (extra-ordinary) due to propagation in the magnetosphere of the pulsar. Even the cause for the slight non-orthogonality has been addressed by investigators like Petrova (2001).

In this paper, after briefly describing the details of our observations in Sec. 2, we summarize the conventional approach to RM determination in Sec. 3. Here we describe the aforementioned RM variations as a function of pulse longitude for PSR B2016+28. In Sec 4 & 5 we show how quasi-orthogonal modes in pulsars can cause severe artifacts in RM estimations, and in particular how the apparent variations in the RM of PSR B2016+28 can be produced. We conclude our analysis with a detailed discussion in Sec. 6. The symbols for variables used in this paper are defined in the appendix.

## 2. Observations

The average pulse observations were performed at the Arecibo Observatory at 430 MHz in May and December 1992 with a band width of 5 MHz. Average pulse profiles were produced by integrating the signal in each frequency channel for 120 seconds. The observation setup has been described in detail in Weisberg et al. (2003).

The single-pulse observations were carried out

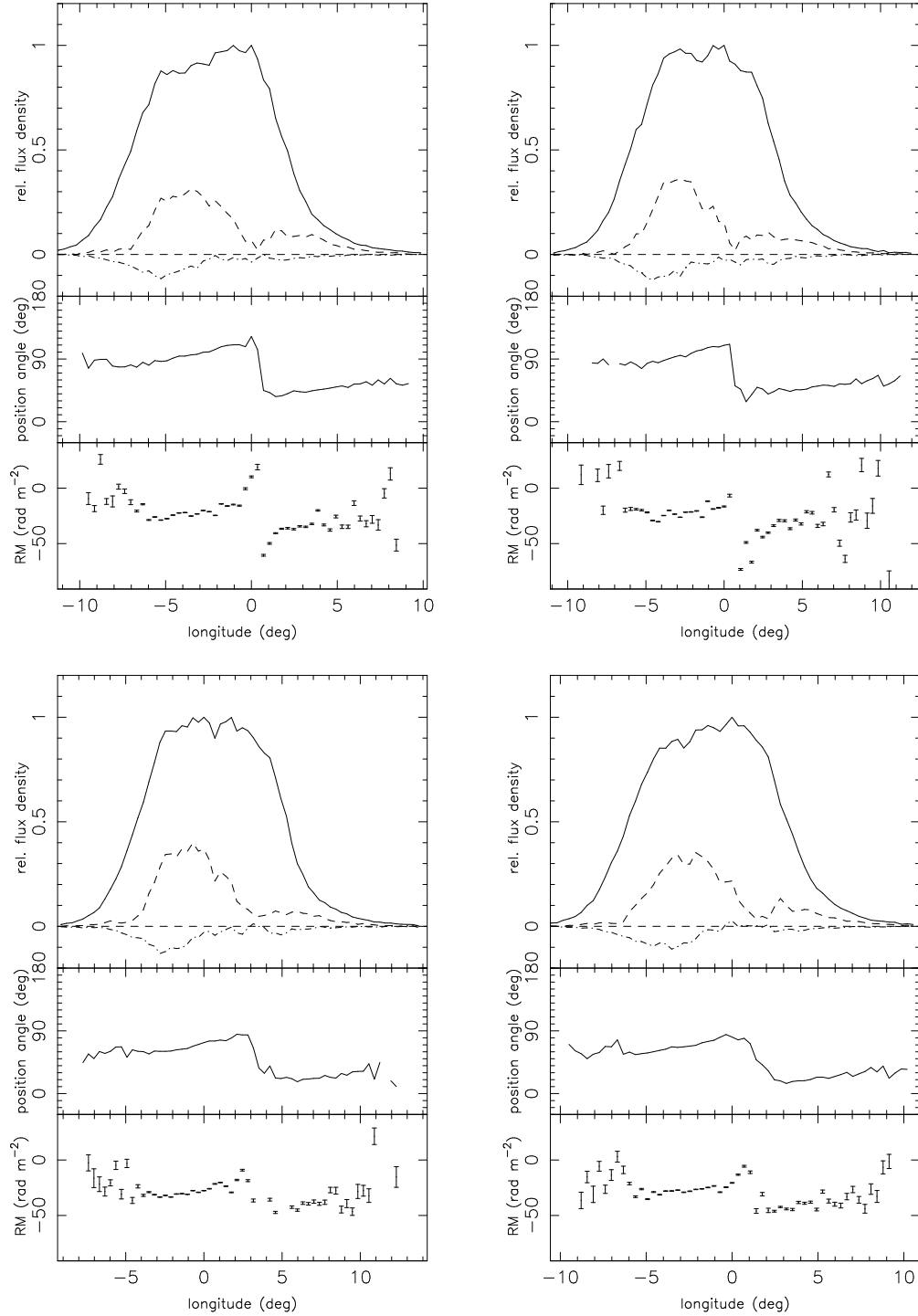


Fig. 1.— (a) – (d) : Results from four different average-pulse data sets. Top panel gives the average profile in Stokes I parameter (solid line), linearly polarised power (‘dash’ line) and circularly polarised power (‘dot-dash’ line). **Middle:** Linear polarisation position angle determined from the average profile. **Bottom:**  $RM(\phi)$  vs  $\phi$ . See text for details.

at Arecibo Observatory at 430-MHz centre frequency in a single session on October 1992. With a special program for gating the 40-MHz correlator, auto-correlation and cross-correlation functions of the right-hand and left-hand polarisation-channel voltages were recorded with 32 correlation lags. The bandwidth of the observation was 10 MHz. The correlation vectors were averaged to a time resolution of 506  $\mu\text{sec}$ . The correlation data were three-level corrected after scaling, and Fourier transformed to produce Stokes parameter spectra. A detailed calibration procedure was adopted to correct for instrumental effects, delays and interstellar dispersion. These observations as well as calibration procedures have been described in Rankin & Rathnasree (1995). The resulting polarised pulse sequence had 32 channels (although channel 1 lacked Stokes U and thus was unusable) with 3043 pulses (1600 sec), and was gated to include a longitude range of some  $45^\circ$ . A constant RM value of  $-34.6 \text{ rad m}^{-2}$  (earlier measurement in the literature) was also subtracted from the data.

### 3. Conventional RM measurements

As individual pulses from pulsars are in general faint, one typically generates an ‘‘average’’ pulse profile by folding the time series in each frequency channel and Stokes parameter synchronously with the Doppler-shifted apparent period. An important property of radio emission from pulsars is that the position angle of linear polarisation changes as a function of pulse longitude (Radhakrishnan & Cooke 1969). Owing to this property, RM measurements of pulsars have always been more complex than for any other polarised radio source in the sky. PA measurements using a given longitude bin of folded profiles and all frequency channels are used to fit for the rotation measure  $[\text{RM}(\phi)]$  on the basis of Eqn. 2. This is repeated for each longitude bin, and the RM from all these bins are averaged to estimate the overall value,  $\langle \text{RM} \rangle$ , for the pulsar. Of course, the underlying assumption here is that the value measured in all the longitude bins are entirely introduced by only the interstellar medium, and hence there is no longitude-dependent Rotation Measure introduced by the pulsar itself. Errors in the  $\text{RM}(\phi)$  can be simply propagated using the S/N of each individual estimate and an assumption of independence of the

estimates.

In our analysis, as the first step, we have attempted to compute  $\text{RM}(\phi)$  values as a function of pulse longitude. As mentioned above, this has been estimated from the average profiles constructed in each of the 31 frequency channels in our sequence. Fig. 1 & 2 summarise the results. Fig. 1 shows the results from four different scans from our, each of 120 sec integration. In the top panel, we give average pulse profile in Stokes I parameter (solid line), average linearly polarised power (‘dash’ line), and average circularly polarised power (‘dot-dash’ line). The middle panel shows linear polarisation position angle, and the bottom panel shows  $\text{RM}(\phi)$ .

In the top panel of Fig. 2, the solid line gives the average pulse profile in total power and the ‘thin’ dash line gives the average profile in linear polarisation computed from average profiles in all Stokes parameters. This is to be compared with the ‘thick’ dash line, which gives linear power computed from single-pulses and averaged over all pulses. As we can see, the ‘thin’ dash line shows a smaller degree of linear polarisation owing to incoherent superposition of the polarisation modes. Then the ‘thin’ dot-dash line indicates power in circular polarisation computed from average profiles in Stokes-V parameter. Power less than zero just means that it is left-circularly polarised.

The dots in the middle panel give the linear polarisation PA curve as defined by the average profile, and the gray scale gives the probability density function (PDF) of the position angle computed from all the single-pulses. While computing this PDF, we have weighted the values with the square of their S/N ratio of the polarised flux as defined by  $\sqrt{Q^2 + U^2}/\sigma_{\text{sys}}$  (where  $Q$  &  $U$  are two of the Stokes parameters, and  $\sigma_{\text{sys}}$  is the root-mean-square value of the system noise flux<sup>2</sup>). Although the PA range outside  $\pm 90^\circ$  is redundant, we have chosen a range of  $\pm 180^\circ$  for clarity.

In the bottom panel of Fig. 2, we give the measured values of  $\text{RM}(\phi)$  as a function of pulse longitude. The dotted line in the bottom panel shows the earlier measurement of RM for this pulsar

<sup>2</sup>As the telescope gain of Arecibo Telescope is significantly high, variation of system noise with the strength of the pulsar was explicitly taken into account with the help of calibrated average pulse profile.

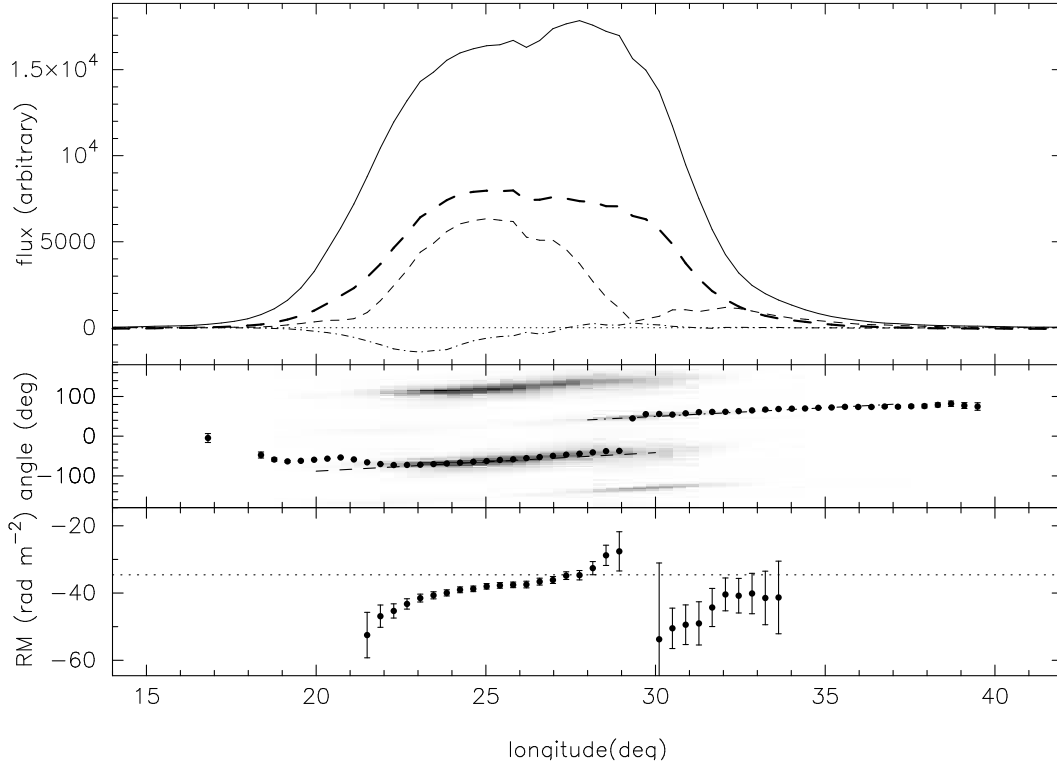


Fig. 2.—  $\text{RM}(\phi)$  vs  $\phi$ . **Top** : Average pulse profile in Stokes-I is given as solid line. ‘Thin’ and ‘thick’ dash lines are linear polarisation power computed from average pulses and from single-pulses and averaged over all pulses, respectively. ‘Thin’ dot-dash line gives circular polarisation power (Stokes V) computed from average pulses. A horizontal dotted line is drawn to indicate the zero-level in the Y-axis. **Middle** : The dots show position angle estimated from the average profile. The gray scale gives the probability density function of position angles estimated from single-pulses. **Bottom** :  $\text{RM}(\phi)$  estimated from average pulse. The value of  $\langle \text{RM} \rangle$  computed from this is  $-38.3(3)$   $\text{rad m}^{-2}$ .

(Manchester 1972),  $-34.6 \text{ rad m}^{-2}$ . As we mentioned in Section 2, the data that we used for our analysis already had a constant RM value of  $-34.6 \text{ rad m}^{-2}$  removed from it. But to be consistent, we have added this offset in the plot (dotted line). Effective RM from our measurement comes to  $-38.3(3) \text{ rad m}^{-2}$ , which is significantly different from the earlier measurement of Manchester, as well as of Weisberg et al. (2003), which is  $-27.3 \pm 2.1 \text{ rad m}^{-2}$ .

There are two aspects of Fig. 1 & 2 that needs to be discussed here. The measured values of  $\text{RM}(\phi)$  as a function of pulse longitude display significant systematic variations. If this effect is true, then it has a very fundamental significance, as one does not expect the interstellar medium to distinguish

between one pulse longitude to the other. Therefore, this RM difference must be due to intrinsic propagation effects in the pulsar magnetosphere. In fact, this would become the first ever direct evidence for propagation effects in the pulsar magnetosphere. However, as we will show in the following section, this is due to artifacts introduced by superposition of the two more or less orthogonal emission modes seen in this pulsar.

Secondly, in Fig. 1, the overall behaviour of  $\text{RM}(\phi)$  is similar in all plots. As described in Sec. 2, these data sets were obtained in May and December 1992. The ‘anti-symmetric’ behaviour of  $\text{RM}(\phi)$  (with respect to longitude value of zero in Fig. 1) seems to be stable over a time scale of several months. However, although the overall be-

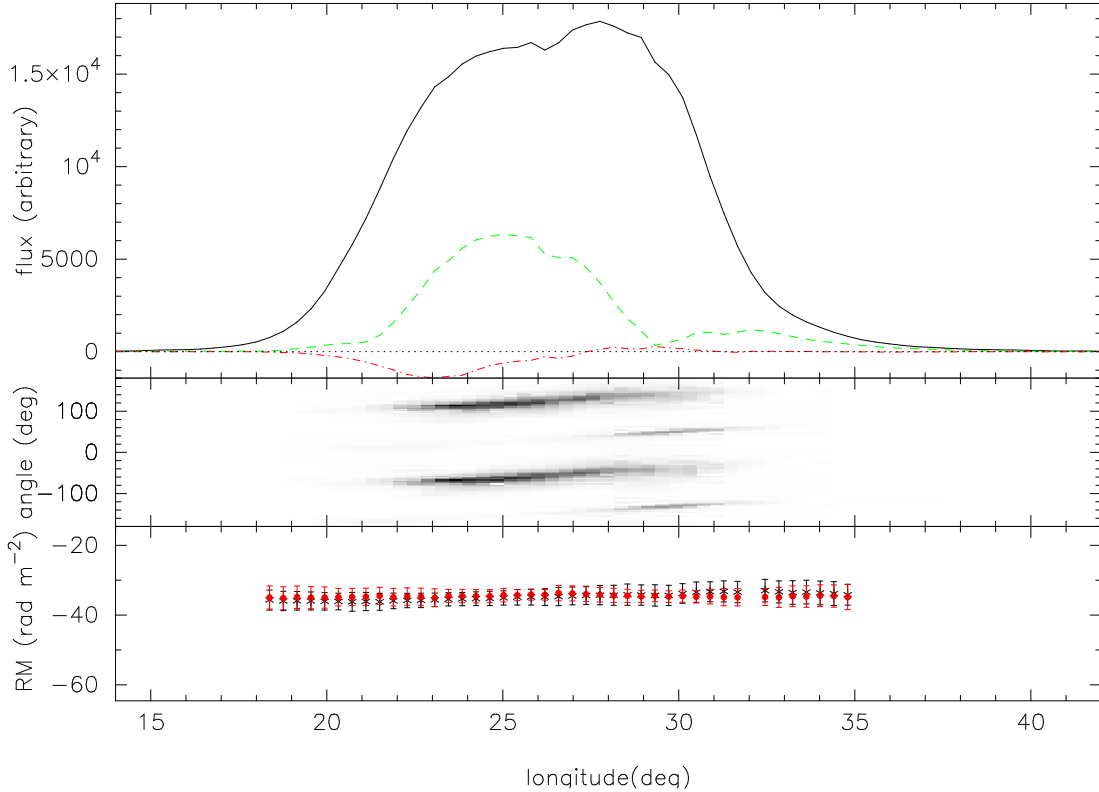


Fig. 3.— Rotation Measure of the two polarisation modes [ $\mathcal{RM}_A(\phi)$  &  $\mathcal{RM}_B(\phi)$ ] as a function of pulse longitude. For comparison, we have given average profiles in total power (solid), linear (dash) and circular (dotted) polarisation in the top panel, and position angle PDF in the middle panel as gray scale. The bottom panel gives the Rotation Measure of the two modes,  $\mathcal{RM}_A(\phi)$  and  $\mathcal{RM}_B(\phi)$ . Effective values of RM of the two modes are  $-35.0(4)$  &  $-34.5(3)$   $\text{rad m}^{-2}$ .

behaviour of  $\text{RM}(\phi)$  is stable, it is quite clear that the exact value of  $\text{RM}(\phi)$  is not the same in all the panels of Fig. 1. We will return to this later in Sec. 6.

RM values varying as a function of pulse longitude is not unique to this pulsar alone. It turns out that this has been observed in other pulsars like PSR B0329+54 (Mitra, Johnston & Kramer, private communication).

#### 4. Intrinsic $\text{RM}(\phi)$ variations?

If the two polarisation modes are strictly orthogonal, then they have no effect on conventional RM measurements. When we compute the average profile in each frequency channel, all that we are doing is “incoherently” superposing the radiation from the two orthogonal modes. This would

mean that the net degree of polarisation is the difference of their degrees of polarisation, and the PA direction is the same as that of the dominant mode. Provided adequate resultant polarised signal, we can still estimate the RM value. If the modes are not strictly orthogonal, then the net PA of the average is the result of a vector summation. This too is of no consequence to RM determination as long as the relative strength of the two modes and their individual mean PA remain constant as a function of radio frequency.

There have been only a few quantitative studies of the frequency dependence of the orthogonal modes (Karastergiou 2002; 2003). In general the degree of polarization of this pulsar decreases significantly with increasing frequency (Gould & Lyne 1998). Also, as the observations of Gould &

Lyne show, the mode-dominance transition point (longitude of  $\sim 29^\circ$  in Fig. 2) moves to earlier longitudes with increasing radio frequency. This indicates that the relative strengths of the modes *do not* remain constant as a function of frequency. In other words, the first half of the profile, which is predominantly polarised with mode-A (represented by a dash line) has a steeper spectral index when compared to the second half that is predominantly polarised with mode-B (dot-dash line).

In the case of PSR B2016+28, it is also clear that the modes are not exactly orthogonal. The best fit to the two gray-scale tracks show that the PA and the slope at  $30^\circ$  longitude are :  $-42^\circ.8(2)$  and  $5.04(1)^\circ/^\circ$  for mode-A (represented by the dash line) and  $49^\circ.8(1)$  and  $4.37(1)^\circ/^\circ$  for mode-B (dot-dash line). These two slope values are significantly different from each other. This PA non-orthogonality is known in the literature (Gil, Snakowski & Stinebring 1991; Gil et al. 1992), and has recently been studied in detail by McKinnon (2003). In fact, it has been shown by McKinnon that this is fairly common among several pulsars (e.g. PSRs B0950+08, B1929+10, B2020+28).

### 5. RM determination in presence of quasi-orthogonal modes

Although the fractional polarisation seen in the average pulse profiles are typically a few tens of percent, individual pulses can exhibit even higher degree of polarisation, some times nearly reaching hundred percent (Stinebring et al. 1984; Rankin et al. 1989; Ramachandran et al. 2002; Rankin & Ramachandran 2003). Given the presence of the quasi-orthogonal modes and possible depolarisation due to their superposition, quite independent of any possible artifacts, it makes sense for us to determine the RM with individual pulses rather than average pulses.

As described in Section 2, our single pulse data set of PSR B2016+28 consists of 3843 pulses, gated to represent a longitude range of about  $45^\circ$  in each pulse. As the first step, in each frequency channel, we produced a PA distribution for every longitude. In doing this, we weighted each sample by the square of S/N of the polarised flux. At a given longitude, due to the presence of the two modes, one expects two significant peaks in this distribution separated by almost  $90^\circ$ .

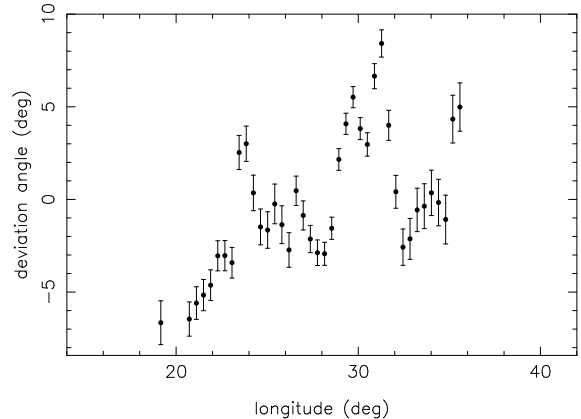


Fig. 4.— Average deviation angle (Y-axis) from non-orthogonality of the two polarisation modes as a function of pulse longitude (X-axis). See text for details.

As the second step, by a weighted mean, we found the centroid of the two peaks [ $\chi_A(\phi, \nu)$  and  $\chi_B(\phi, \nu)$ ], both being functions of pulse longitude and radio frequency. We thus determined the mean PA values of each mode.

Once the PAs are determined, then it is straight forward to fit for rotation measure values of the two modes,  $\mathcal{RM}_A(\phi)$  and  $\mathcal{RM}_B(\phi)$ , as a function of pulse longitude. These two functions determined for PSR B2016+28 are given in Fig. 3. Comparing this to the bottom panel of Fig. 2, it is obvious that the deviations of RM values observed for the two modes is far less than what is determined with the average profiles. The effective RM values of the two modes turn out to be  $-35.0 \pm 0.4$  and  $-34.5 \pm 0.3$   $\text{rad m}^{-2}$ , respectively. These values are very close to the earlier measurement of  $-34.6 \pm 1.4$   $\text{rad m}^{-2}$  (Manchester 1972).

As emphasised in Section 4, the presence of the two modes itself, even if they are not orthogonal, should not introduce any artifact in RM measurements, as long as there is no frequency dependence of the relative strength and the intrinsic PAs of the two modes. However, in our analysis of PSR B2016+28, the value of  $\text{RM}(\phi)$  is significantly different from the values of  $\mathcal{RM}_A(\phi)$  and  $\mathcal{RM}_B(\phi)$ , which clearly indicates that the incoherent superposition of the modes while generating average profiles (as a function of frequency) has introduced a frequency dependence of the re-

sultant PA , which manifests as *extra* RM.

To investigate this subtle effect in detail, with the help of the above described procedure, we produced Fig. 4, that shows the non-orthogonality of the two modes as a function of pulse longitude. We have plotted the quantity

$$\Delta\psi(\phi) = \frac{\pi}{2} - \langle [\chi_B(\phi, \nu) - \chi_A(\phi, \nu)] \rangle_\nu. \quad (3)$$

against pulse longitude ( $\phi$ ). As we can see, the deviations are not uniform across the pulse profile, and the variations are statistically significant.

Let  $X_A(t, \nu)$  and  $X_B(t, \nu)$  be the “instantaneously” randomly varying linearly polarised intensities of the two quasi-orthogonal modes. Let  $\zeta(\nu)$  be the angle between the two vectors in the Stokes Q–U space. Assuming that the PA of the primary mode is zero, we can write the two Stokes parameters  $Q$  and  $U$  as (see also McKinnon 2003)

$$\begin{aligned} Q(t, \nu) &= X_A(t, \nu) + X_B(t, \nu) \cos \zeta(\nu) + X_Q(t, \nu) \\ U(t, \nu) &= X_B(t, \nu) \sin \zeta(\nu) + X_U(t, \nu) \end{aligned} \quad (4)$$

If  $\zeta(\nu)$  is independent of  $X_A(t, \nu)$ , then the PA as a function of frequency with average values of  $Q$  and  $U$  is

$$\begin{aligned} \langle \chi_{AB}(\nu) \rangle &= \frac{1}{2} \tan^{-1} \left[ \frac{\langle U(t, \nu) \rangle}{\langle Q(t, \nu) \rangle} \right] \\ &= \frac{1}{2} \tan^{-1} \left[ \frac{\sin \zeta(\nu)}{F_{AB}(\nu) + \cos \zeta(\nu)} \right] \end{aligned} \quad (5)$$

where the angular brackets indicate time-averaging, and  $F_{AB}(\nu) = \langle X_A(t, \nu) \rangle / \langle X_B(t, \nu) \rangle$ .  $X_Q(t, \nu)$  and  $X_U(t, \nu)$  are the system noise strengths in  $Q$  and  $U$  as a function of time and frequency. As we can see, in principle, frequency dependence in  $\zeta(\nu)$  or  $F_{AB}(\nu)$  can introduce a frequency dependent  $\langle \chi_{AB}(\nu) \rangle$ , which can corrupt our rotation measure determination.

The dependence of  $\langle \chi_{AB}(\nu) \rangle$  on frequency is different from that of the RM. Therefore, in principle, the RM measured at different frequency ranges should be different. To check this, we divided our frequency band into two parts. Indeed, the value of  $\text{RM}(\phi)$  was different in the two halves. In the first half of the band, the measured value of RM was  $-32.5(9)$  rad m<sup>-2</sup>, whereas in the other it was  $-40.5(4)$  rad m<sup>-2</sup>. The overall value of  $\langle \text{RM} \rangle$  was  $-38.3(6)$  rad m<sup>-2</sup>.

The error introduced by this effect depends on the bandwidth, centre frequency, frequency dependences of  $\zeta(\nu)$  and  $F_{AB}(\nu)$ . Fig. 5 succinctly summarises this effect. This theoretically generated plot corresponds to a centre frequency of 430 MHz and a band width of 10 MHz, which is divided into 128 frequency channels. In the left panel, we give  $\zeta(\nu)$  in the X-axis and effective RM introduced by this quasi-orthogonal mode-mixing in the Y-axis. The five curves, *solid*, *dash*, *dot-dash*, *dotted* and *dot-dot-dot-dash*, correspond to variations of fractional strength of the two modes [ $F_{AB}(\nu)$ ] from the lower to the upper end of the frequency band of 0.3–0.9, 0.45–0.9, 0.6–0.9, 0.75–0.9 and a constant 0.9, respectively. As is seen, when the relative strength remains constant, then the RM introduced by this effect is zero. However, when the relative strength varies as a function of frequency, then the spurious RM introduced in the measurement could be significant.

In the right panel of Fig. 5, we have addressed the other possibility that for a constant fractional strength across the frequency band,  $\zeta(\nu)$  varies. The five curves, *solid*, *dash*, *dot-dash*, *dotted* and *dot-dot-dot-dash*, correspond to  $\zeta(\nu)$  varying in the ranges of 160°–180°, 165°–180°, 170°–180°, 175°–180°, and a constant value of 180°, respectively. Here, the RM value changes sign at  $F_{AB}(\nu) = 1$ , and this is exactly what we see in Fig. 2. The inferred value of  $\text{RM}(\phi)$  has an anti-symmetry with respect to  $\phi \sim 30^\circ$ , where one mode is stronger to the right and the other mode to the left. It is worth noting here that in Fig. 5, at the limit of  $F_{AB}(\nu) \rightarrow \infty$ , the RM introduced asymptotically reduces to zero.

## 6. Discussion

In Fig. 1 & 2, one of the intriguing things is that the value  $\text{RM}(\phi)$  does not remain constant between various epochs of observation. Perhaps one of the reasons could be a combination of interstellar scintillation and the effect that we have addressed in this paper. Although scintillation is not expected to have any effect on the amount of Faraday rotation introduced in the interstellar medium, when the total integration time is short ( $\sim$  a few minutes), the effective centre frequency and bandwidth is expected to vary. Combined with the effect that we have described, the RM



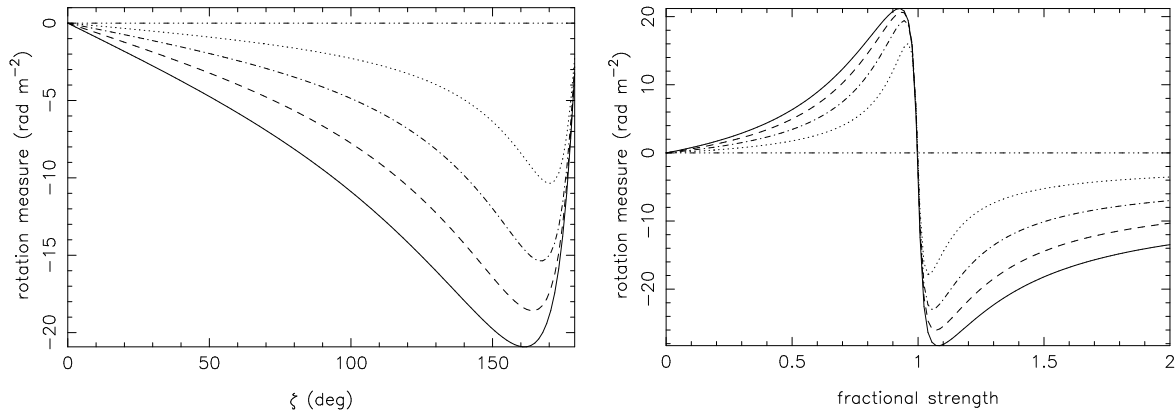


Fig. 5.— Effective RM introduced by non-orthogonal mode-mixing (Y-axis). Left panel shows RM as a function of  $\zeta(\nu)$ . For a constant  $\zeta(\nu)$  value, the five curves, *solid*, *dash*, *dot-dash*, *dotted* and *dot-dot-dot-dash*, correspond to variations of fractional strengths of the two modes ( $F_{AB}(\nu)$ ) from the lower to the upper end of the frequency band of 0.3–0.9, 0.45–0.9, 0.6–0.9, 0.75–0.9 and a constant 0.9, respectively. In the right panel, the five curves correspond to the variation of  $\zeta(\nu)$  of  $160^\circ$ – $180^\circ$ ,  $165^\circ$ – $180^\circ$ ,  $170^\circ$ – $180^\circ$ ,  $175^\circ$ – $180^\circ$ , constant value of  $180^\circ$ , respectively. See text for details.

value inferred in principle can be different at different epochs. Moreover, as described in Sec. 2, each of the four panels (a to d) in Fig. 1 has been produced with 120 second ( $\sim 200$  pulses) long scans. Pulsars are known to exhibit stable average-pulse profiles only after integrating a few thousands of pulses. As we can see from the four panels, average profiles, and even polarisation-sweep curves, are not identical between all the panels. This may also introduce time-dependence in RM values.

As mentioned in Sec. 5, the exact frequency dependence of  $F_{AB}(\nu)$  and  $\zeta(\nu)$  are not known. In general, there is no reason to conclude that the frequency dependence of  $\langle \chi_{AB}(\nu) \rangle$  introduced by this effect is the same as that of the RM. What we have attempted in Fig. 5 is to estimate the effective RM introduced by this effect. A thorough investigation of the nature of the emission modes and their frequency dependence is beyond the scope of this publication, and we plan to consider these matters in a subsequent report.

As radiation from pulsars is highly polarised and as distance estimates to pulsars are more reliable than the other polarised sources (e.g. supernova remnants), pulsar RM determinations have been used extensively in probing the magnetic field structure of the Galaxy. RM is an important tool

to model the long range as well as the turbulent component of the magnetic field in the Galaxy. If the effect that we have discussed in this paper is common, then it will have serious consequences on the existing RM measurements of pulsars, and thereby on the models of magnetic field structure in the Galaxy. Apart from our detailed analysis of PSR B2016+28 presented here, in the sample of Weisberg et al. (2003), we looked at pulsars B0301+19, B0525+21, B0626+24, B1929+10 and B2020+28. These all showed systematic variation of the RM across the pulse profile. For instance, Weisberg et al. measure RM values for these pulsars as  $-5.7 (\pm 10)$ ,  $-39.2 (\pm 10)$ ,  $69.5 (\pm 10)$ ,  $-5.9 (\pm 5)$ ,  $-73.7 (\pm 25)$  rad m $^{-2}$ , respectively. The values given in parenthesis are the approximate magnitude of variations seen around the mean value across the pulse profile. As we can see clearly, these variations are significant. Especially, when the magnitude of RM is small, these variations can cause significant bias.

The presence of orthogonal modes is common among pulsars. Among pulsars for which any amount of detailed single-pulse study has been done so far, it is clear that a great majority of them exhibit orthogonal modes. In particular, it is almost impossible to find a “conal” pulsar that does not show evidence of orthogonal mode emission

associated with its conal components (Rankin & Ramachandran 2003). It is also possible that these two modes have significantly different spectral indices. For instance, there is clear evidence to show that the degree of polarisation in the average-pulse profiles decreases with increasing frequency. This can be understood easily by having one of the modes dominating in strength at lower frequencies, and the two modes having roughly comparable strengths at very high frequencies. As the earlier studies (Stinebring et al. 1984; Gil, Snakowski & Stinebring 1991; Gil et al. 1992; McKinnon 2003) have shown, these modes are slightly non-orthogonal, and this non-orthogonality of the two modes is a wide-spread phenomenon.

As we have shown in this paper, the only way to eliminate this artifact is to determine RM values from single pulses. This, of course, is a very challenging task, owing to signal-to-noise ratio considerations. For weaker pulsars for which we cannot obtain good single pulse data, it is impossible to separate the two modes to unambiguously determine RM values. Therefore, weaker pulsars are bound to suffer from this artifact, and there is no obvious way of correcting it.

On the Galactic scale, whether or not this effect will make serious changes to the magnetic field model, remains to be seen. A project to determine correct RM values for several other pulsars is underway, and will be presented in a subsequent publication. It is conceivable that this artifact will be most prominent among pulsars with small RM magnitudes ( $\leq 50$  rad  $m^{-2}$  or so). A thorough analysis to check the validity of the already existing RM values, and the effect on the Galactic magnetic field structure is much needed.

## 7. Conclusion

Our major conclusions from this work can be summarised as follows:

- We find that the rotation measures determined for PSR B2016+28 as a function of pulse longitude varies significantly. This seems to be the case for five other pulsars, namely PSRs B0301+19, B0525+21, B0626+24, B1929+10 and B2020+28.
- This effect is an artifact introduced by the frequency dependence of relative strengths

of the two modes as well as the amount of non-orthogonality, and it is not intrinsic to the pulsar magnetosphere. We show that if we estimate rotation measure for the two modes separately, this effect can be removed. The technique to remove this artifact invariably involves analysis with single pulses. Hence, cannot be carried out for fainter objects. There is no other obvious way of compensating for this artifact for these fainter objects.

- As the amount of RM spuriously introduced can be as high as a few tens of units, several measurements of Rotation Measures of pulsars in the literature may be in error, and needs revision.

We thank Jon Arons, Avinash Deshpande, Aris Karastergiou, Simon Johnston, Michael Kramer & Dipanjan Mitra for useful comments on the manuscript. Special thanks are due to Dipanjan Mitra, Simon Johnston and Michael Kramer for sharing their results prior to publication. We also thank our anonymous referee for his/her valuable comments.

## REFERENCES

- Backer, D. C., Rankin, J. M. 1980, ApJS, 42, 143
- Gil, J. A., Lyne, A. G., Rankin, J. M. et al. 1992, A&A, 255, 181
- Gil, J. A., Snakowski, J. A., Stinebring, D. R. 1991, A&A, 242, 119
- Hamilton, P. A., Hall, P. J., Costa, M. E. 1985, MNRAS, 214, 5
- Hamilton, P. A., & Lyne, A. G. 1987, MNRAS, 224, 1073
- Hamilton, P. A., McCulloch, P. M., Manchester, R. N., Ables, J. G., & Komessaroff, M. M. 1977, Nature, 265, 224
- Han, J. L., Manchester, R. N., Qiao, G. J. 1999, MNRAS, 306, 371
- Han, J. L., Manchester, R. N., Lyne, A. G., & Qiao, G. J. 2002, ApJ, 570, 17

- Indrani, C., Deshpande, A. A. 1998, *New Astr.*, 4, 33
- Karastergiou, A., & Johnston, S. 2003, *A&A*, 404, 325
- Karastergiou, A., Kramer, M., Johnston, S., et al. 2002, *A&A*, 391, 247
- Luo, Q., & Melrose, D. B. 1995, *MNRAS*, 276, 372
- Lyne, A. G., Smith, F. Graham 1989, *MNRAS*, 237, 533
- Manchester, R. N. 1972, *ApJ*, 172, 43
- Manchester, R. N. 1974, *ApJ*, 188, 637
- McKinnon, M. 2003, *ApJ*, 590, 1026
- Mitra, D., Wielabinski, R., Kramer, M., & Jessner, A. 2003, *A&A*, 398, 993
- Melrose, D. C. 1979, *Aust. J. Phys.*, 32, 61
- Petrova, S. A. 2001, *A&A*, 378, 883
- Petrova, S. A., & Lyubarskii, Y. E. 2000, *A&A*, 355, 1168
- Qiao, G. J., Manchester, R. N., Lyne, A. G. & Gould, D. M. 1995, *MNRAS*, 274, 572
- Radhakrishnan, V., & Cooke, D. J. 1969, *Astrophys. Lett.*, 3, 225
- Radhakrishnan, V., & Deshpande, A. A. 2001, *A&A*, 379, 551
- Ramachandran, R., Rankin, J. M., Stappers, B. W., Kouwenhoven, M. L. A., van Leeuwen, A. G. J. 2002, *A&A*, 381, 993
- Rand, R. J., & Lyne, A. G. 1994, *MNRAS*, 268, 497
- Rankin, J. M., Campbell, D. B., Isaacman, R. B., Payne, R. R. 1988, *A&A*, 202, 166
- Rankin, J. M., & Ramachandran, R. 2003, *ApJ*, 590, 411
- Rankin, J. M., Stinebring, D. R., & Weisberg, J. M. 1989, *ApJ*, 346, 869
- Rankin, J. M., Rathnasree, N. 1995, *JApA*, 16, 327
- Stinebring, D. R., Cordes, J. M., Weisberg, J. M., Rankin, J. M., & Boriakoff, V. 1984, *ApJS*, 55, 247
- Thompson, R. C., & Nelson, A. H. 1980, *MNRAS*, 191, 863
- Weisberg, J. M., Cordes, J. M., Kuan, B. et al., 2003, *ApJ Supp*, in press (astro-ph/0310073)

---

This 2-column preprint was prepared with the AAS L<sup>A</sup>T<sub>E</sub>X macros v5.0.

## DEFINITIONS

Variable	Definition
$\phi$	pulse longitude
PA	linear polarisation position angle
RM	Rotation Measure
$\text{RM}(\phi)$	Rotation Measure at a given longitude $\phi$ measured with average pulse profiles.
$\mathcal{RM}_A(\phi)$	Rotation Measure of polarisation mode-A
$\mathcal{RM}_B(\phi)$	Rotation Measure of polarisation mode-B
SNR	signal-to-noise ratio
$\chi_A(\phi, \nu), \chi_B(\phi, \nu)$	Weighted mean values of linear polarisation position angles of Mode-A and Mode-B
$\langle \chi_{AB}(\nu) \rangle$	linear polarisation position angle at a given frequency after incoherently superposing the two (non-)orthogonal modes.
$X_A(t, \nu), X_B(t, \nu)$	linear polarisation intensities of the two modes as a function of time and frequency.
$X_N(t, \nu)$	system noise power as a function of time and frequency.
$\langle \text{RM} \rangle$	Net RM value computed from average pulse profile after averaging over all pulse longitudes.